J Nanopart Res (2013) 15:1860
DOI 10.1007/s11051-013-1860-6

RESEARCH PAPER

Polyinosinic:polycytidylic acid loading onto different generations of PAMAM dendrimer-coated magnetic nanoparticles

Rouhollah Khodadust · Pelin Mutlu · Serap Yalcın · Gozde Unsoy · Ufuk Gunduz

Received: 7 April 2013 / Accepted: 11 July 2013 / Published online: 30 July 2013

Abstract Poly (I:C), which is a synthetic double-stranded RNA, have significant toxicity on tumor cells. The immobilization of Poly (I:C) onto nanoparticles is important for the fabrication of targeted delivery systems. In this study, different generations of newly synthesized PAMAM dendron-coated magnetic nanoparticles (DcMNP) which can be targeted to the tumor site under magnetic field were efficiently loaded for the first time with Poly (I:C). Different generations of DcMNPs (G_2, G_3, G_4, G_5, G_6, and G_7) were synthesized. Poly (I:C) activation was achieved in the presence of EDC and 1-methylimidazole. Loading of Poly (I:C) onto DcMNPs was followed by agarose gel electrophoresis. Acidic reaction conditions were found as superior to basic and neutral for binding of Poly (I:C). In addition, having more functional groups at the surface, higher generations (G_7, G_6, and G_5) of PAMAM DcMNPs were found more suitable as a delivery system for Poly (I:C). Further in vitro and in vivo analyses of Poly (I:C)/PAMAM magnetic nanoparticles may provide new opportunities for the selective targeting and killing of tumor cells.

Keywords Poly (I:C) · Magnetic nanoparticles · Targeted delivery system · Cancer therapy

R. Khodadust · G. Unsoy · U. Gunduz
Department of Biotechnology, Middle East Technical University, 06800 Ankara, Turkey

R. Khodadust (✉) · U. Gunduz (✉)
Department of Biological Sciences, Middle East Technical University, 06800 Ankara, Turkey
e-mail: raoul.1357@gmail.com

U. Gunduz
e-mail: ufukg@metu.edu.tr

P. Mutlu
Central Laboratory, Molecular Biology and Biotechnology R&D Center, Middle East Technical University, 06800 Ankara, Turkey

S. Yalcın
Department of Food Engineering, Ahi Evran University, 40000 Kırşehir, Turkey

Introduction

Most pharmacological approaches to cancer therapy are based on standard chemotherapy protocols which generally exhibit high cytotoxicity and poor specificity (Dobson 2006; Sun et al. 2008; Colombo et al. 2012). Magnetic nanoparticles (MNPs) based on iron oxide are being used in clinical applications as targeted drug delivery system in the recent years. By the help of an implanted permanent magnet or an externally applied field, they can be targeted to the tumor side resulting in the accumulation of the drug (Colombo et al. 2012; Widder et al. 1979).

In order to became an effective drug carrier system, MNPs should be firstly coated with a suitable polymer shell such as PEG, dextran, chitosan, polyethyleneimine, and PAMAM dendrimer (Colombo et al. 2012;

Unsoy et al. 2012; Kohler et al. 2004; Shen et al. 1993; Ho and Li 2008; McBain et al. 2007). The resulting MNPs then can circulate in the blood for a long period of time without being cleared (Mornet et al. 2004). Finally, loading these MNPs with targeting ligands having high selectivity for specific cancer cell receptors make them functional (Veiseh et al. 2010).

PAMAM dendrimers are synthesized that produces concentric shells of branch cells (generations) around a central initial iron oxide core (Bosman et al. 1999). The PAMAM dendrimers have primary amine groups at each branch end and tertiary amine groups at each branching point (Maiti et al. 2005). The terminal amine groups of PAMAM dendrimers can be modified with different functionalities and can be linked with various biomolecules such as drugs, antibodies and imaging agents (Patri et al. 2002). The bioactive agents may either be encapsulated into the interior of the dendrimers or they may be chemically attached or physically adsorbed onto the dendrimer surface (Svenson and Tomalia 2005).

Successful immunization against pathogens or cancer cells results in the activation of adaptive immunity, in part, through stimulation of the Toll-like receptors (TLRs) (Takeda et al. 2003; Shukoor et al. 2007). TLRs are a class of proteins that play a key role in the innate immune system (Hansson and Edfeldt 2005). It has been estimated that most mammalian species have between ten and fifteen types of Toll-like receptors (Du et al. 2000; Tabeta et al. 2004). Well-conserved features in pathogens such as bacterial cell surface lipopolysaccharides, flagellin, double-stranded RNA of viruses, and the unmethylated CpG islands of bacterial and viral DNA are the ligands of the TLRs (Hemmi et al. 2000). Viral single- or double-stranded RNA is recognized by TLR3 receptor (Shukoor et al. 2007; Schulz et al. 2005).

Polyinosinic:polycytidylic acid (Poly I:C), being an immunostimulant, is a synthetic analog of double-stranded RNA which exerts its function via TLR3 (Salaun et al. 2009; Salvador et al. 2012). It is a potent interferon inducer and can activate monocytes and natural killer cells to produce pro-inflammatory cytokines and chemokines (Salvador et al. 2012; Salem et al. 2006). Poly (I:C) can directly trigger apoptosis in many types of human malignant cells including breast cancer, melanoma and hepatoma cells by activating TLR3(Khvalevsky et al. 2007; Weber et al. 2010; Xiangzhong et al. 2012). The TLR3 is primarily expressed in intracellular vesicles such as the endoplasmic reticulum, endosomes, and lysosomes (Matsumoto et al. 2004; Kawai and Akira 2010). TLR3 signaling, which is induced by Poly (I:C), is mediated by the TIR domain-containing adaptor-inducing interferon-β (TRIF) adaptor molecule through the TRIF-dependent pathway. TRIF is responsible for the activation of interferon regulatory factor 3 (IRF-3) and NF-κB and the induction of type I IFN (Matsumoto et al. 2004; Kawai and Akira 2010). On the other hand, retinoic acid inducible gene I (RIG-I) and melanoma differentiation-associated gene 5 (MDA-5) are cytosolic RNA sensors (Xiangzhong et al. 2012; Kato et al. 2006). RIG-1 and MDA-5 bind with IFN-β promoter stimulator 1 (IPS-1) which is located in the outer mitochondrial membrane activates type I IFN and NF-κB (Kawai et al. 2005; Kumar et al. 2006). Poly (I:C) shows antitumor and antiviral activity and recently entered into phase II clinical trials for patients with malignant gliomas (Shukoor et al. 2007).

When Poly (I:C) is given in vivo, they are rapidly cleared by nucleases so several strategies were proposed as carriers for these kind of nucleic acids attempting to increase their in vivo performances (Borges et al. 2008; Fischer et al. 2009; Schlosser et al. 2008). In cancer therapy, in order to increase the therapeutic efficacy, a triple effector strategy has been developed, combining targeted delivery, apoptosis induction and immunostimulatory properties of the artificial dsRNA Poly (I:C) (Shir et al. 2006; Schaffert et al. 2011). The immobilization of Poly (I:C) onto magnetic nanoparticles is an important tool for the fabrication of targeted delivery systems since they can contribute to precise delivery to an exact target site through the application of external magnetic fields (Shukoor et al. 2007; Whitesides 2003).

In this study, Poly (I:C) was loaded onto different generations of newly synthesized PAMAM dendron-coated magnetic nanoparticles. Loading efficiencies and stabilities of the complex was discussed to evaluate the most effective delivery system in further cancer treatment studies.

Materials and methods

Materials

Ferric chloride hexa-hydrate ($FeCl_3 6H_2O$), ferrous chloride tetra-hydrate ($FeCl_2 4H_2O$), ammonia solution

(NH_3) (32 %), aminopropyltriethoxysilane (APTS) ($NH_2(CH_2)_3$-Si-$(OCH_3)_3$), methylacrylate, methanol, ethanol, ethylenediamine, PBS (Phosphate-buffered saline), EDC (1-ethyl-3-[3-dimethylaminopropyl]carbodiimide hydrochloride), 1-methylimidazole, Polyinosinic-Polycytidylic acid (Poly (I:C)), sodium carbonate were purchased from Sigma-Aldrich and acetic acid was purchased from Merck.

Synthesis of DcMNPs

The magnetic nanoparticles (Fe_3O_4) were prepared by co-precipitation method. $FeCl_24H_2O$ and $FeCl_36H_2O$ (Fe^{+2}: Fe^{+3} = 1:2) were dissolved in distilled water under nitrogen environment and ammonia solution was added slowly with vigorous stirring mechanically at 2,000 rpm for 2 h at 90 °C. The black precipitate was washed five times with distilled water and five times with ethanol using magnetic separation. The obtained iron oxide nanoparticles were dispersed in ethanol (5 g/l) (Khodadust et al. 2013; Pan et al. 2007; Gao et al. 2005; Esfand and Tomalia 2001). Surface modification of Fe_3O_4 was performed with APTS. Ethanol was added into the Fe_3O_4—ethanol solution and sonicated with ultrasonicator (BandelinSonopuls Ultrasonic Homogenizer HD 2200) at 100 % amplitude for 30 min at room temperature. APTS was added to the mixture at twentieth minute of sonication. Then, the mixture was stirred with mechanical stirrer at 2,000 rpm for 15 h at room temperature. The resulting black precipitate was separated by magnetic decantation and washed with methanol for several times. The obtained nanoparticles modified with APTS are called G_0 generation (Khodadust et al. 2013; Pan et al. 2007). Coating of G_0 nanoparticles was carried out with PAMAM dendrimer through Michael reaction (Pan et al. 2007; Gao et al. 2005). Methylacrylate methanol solution (20 %, v/v) was added to the G_0 nanoparticles and the suspension was sonicated in an ultrasonic water bath at room temperature for 7 h. After ultrasonication, nanoparticles were eluted by magnetic decantation and washed with methanol. Ethylenediamine methanol solution (50 %, v/v) was added and suspension was sonicated for 3 h. The particles were washed with methanol. The stepwise growth of dendrons was repeated until the desired number of generation (G_2–G_7) was achieved. The product was then washed three times with methanol and five times with distilled water by magnetic decantation (Khodadust et al. 2013; Pan et al. 2007).The characterization of PAMAM dendron-coated magnetic nanoparticles were performed by X-ray diffraction (XRD), fourier transform infrared spectroscopy (FTIR), thermal gravimetric analysis (TGA-FTIR), and vibrating sample magnetometry (VSM) analyses (Khodadust et al. 2013).

Poly (I:C) activation

The Poly (I:C) products were dissolved in nuclease-free water to a final concentration of 10 mg/ml as stock, yielding a very faint hazy to clear, colorless solution. In order to make bound between 5′-phosphate group of Poly (I:C) and NH_2 groups at the surface of DcMNPs, first Poly (I:C) was heated to 55 °C and then cooled to room temperature to make ds-Poly (I:C) according to manufacturer's procedure (Sigma-Aldrich). Then, the activation procedure was continued in the presence of EDC and 1-methylimidazole (Shukoor et al. 2007, 2008).

Poly (I:C) loading optimization on G_7DcMNP at pH 7, and pH 7.5

G_7DcMNPs were dissolved in 0.1 M 1-methyl-imidazole buffer (pH7) to a final concentration of 10 mg/ml. The EDC solution of 0.013 M was prepared using 0.1 M 1-methyl-imidazole buffer (pH7) and used fresh. Poly (I:C) was diluted as 200 μg/ml in 0.1 M 1-methyl-imidazole buffer (pH7) and 4 μg of Poly (I:C) was put into microcentrifuge tubes. Freshly prepared EDC solution was added immediately and incubated for 15 min at room temperature. Then, G_7DcMNPs/1-methylimidazole solution was added to the reaction with final volume as 100 μl and rotated 2 h at room temperature. The applied PIC:G_7DcMNP ratio/ratios were as 1:10, 1:15, 1:20, 1:30, and 1:35. Poly (I:C)-loaded G_7DcMNPs were washed with distilled water using magnetic separation in order to remove EDC from the solution. The loading procedure of Poly (I:C) also performed on other generations at pH 7, and pH 7.5.

Poly (I:C) loading optimization on G_7DcMNP at pH6

Poly (I:C) loading optimization on G_7DcMNP at pH6 was done by following the similar steps in the "Poly (I:C) loading optimization on G_7DcMNP at pH 7, and

pH 7.5" section. In contradiction, 0.1 M 1-methylimidazole buffer with pH6 was used. In addition, the applied PIC:G_7DcMNP ratio/ratios were as 1:10, 1:11, 1:12, 1:13, and 1:15. After optimization with G_7DcMNP, the loading efficiencies on G_2, G_3, G_4, G_5, and G_6 DcMNPs were also done.

Stability of Poly (I:C) bound DcMNPs

The stabilities of Poly (I:C) on different generations of DcMNPs were studied at different acidic (acetate buffer), basic (carbonate buffer), and neutral (injection buffer and PBS) pH conditions.

Results

DcMNPs synthesis

The magnetic nanoparticles (Fe_3O_4) were prepared with co-precipitation method (Pan et al. 2007). Surface modification of Fe_3O_4 was performed with APTS and the obtained nanoparticles were called G_0 generation (39, 40). Surface coating of G_0 generation of nanoparticles was carried out with PAMAM dendron and the stepwise growth of dendrons was repeated until the desired number of generation (G_2–G_7) was achieved (Fig. 1) (Khodadust et al. 2013).

X-ray photoelectron spectroscopy (XPS), XPS analysis demonstrated that the surface nitrogen atoms appear after aminosilane modification. The percentage of nitrogen atoms exponentially increases by increasing the generation numbers of DcMNPs as amine functional groups at the surface of DcMNPs increases exponentially (Fig. 2).

Characterizations of synthesized DcMNPs by XRD, FTIR, TGA-FTIR, and VSM were previously reported (Khodadust et al. 2013).

Poly (I:C) activation in the presence of EDC and 1-methylimidazole

By the application of carbodiimides/1-methylimidazole, the phosphoramidate linkages were formed between primary amines on the surface of DcMNP and 5′-phosphate of Poly (I:C) molecules. Poly (I:C) first activated by EDC (1-ethyl-3-[3-dimethylaminopropyl] carbodiimide hydrochloride). The immediate addition of 1-methylimidazole causes the release of isourea by-product and formation of reactive phosphorylimidazolide bond between Poly (I:C) and imidazole molecules. In the presence of DcMNPs, the reactive phosphorylimidazolide bond were hydrolyzed and replaced with phosphoramidate bond which was formed between the phosphate groups of Poly (I:C) and surface amine groups of DcMNPs. EDC and imidazole did not become part of the final crosslink between the molecules and thus did not add any additional chemical structure to the resulting products, as a result the reaction by-products

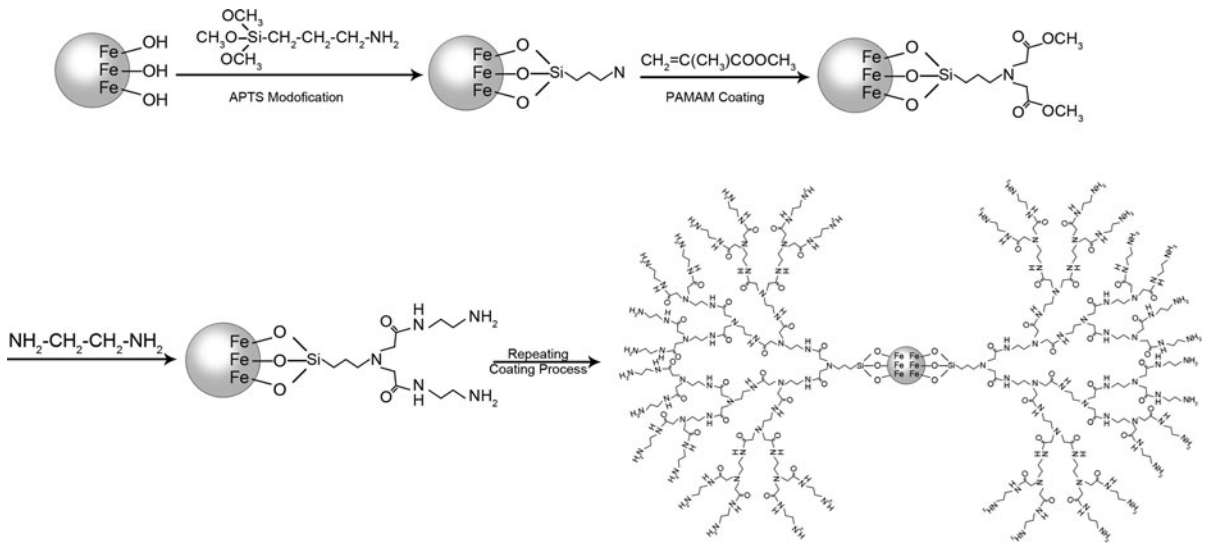

Fig. 1 Stepwise modification of iron oxide nanoparticles with APTS, and dendron coating process

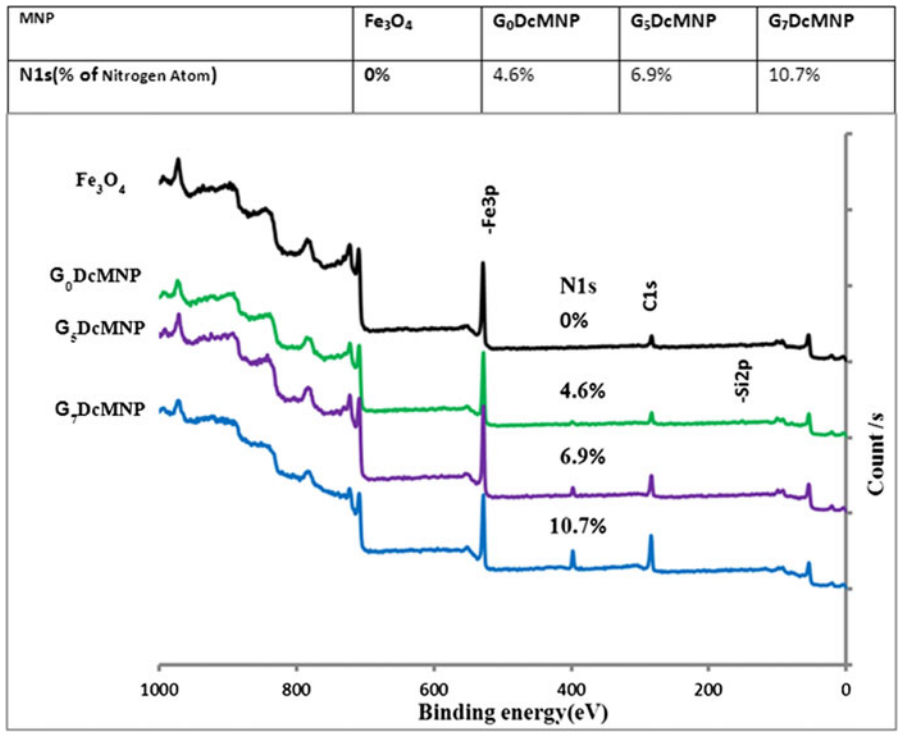

Fig. 2 The X-ray photoelectron spectroscopy (XPS) analysis of Bare MNP, G_0DcMNP, G_5DcMNP, and G_7DcMNP

could be easily removed by magnetic separation (Fig. 3).

Poly (I:C) loading efficiency studies

Poly (I:C) was bound to the surface of DcMNPs in 1-methylimidazole (pH 7.5, pH 7 and pH 6) buffer. Transmission electron microscopy (TEM) and dynamic light scattering (DLS) analyses of G_7DcMNP and Poly I:C-bound G_7DcMNP were shown in Figs. 4 and 5, respectively. TEM analysis of G_7DcMNP show that the nanoparticle size was in the range of 20 ± 5 nm. However, DLS measurement shows the sizes of nanoparticles in the range of 45 ± 10 nm

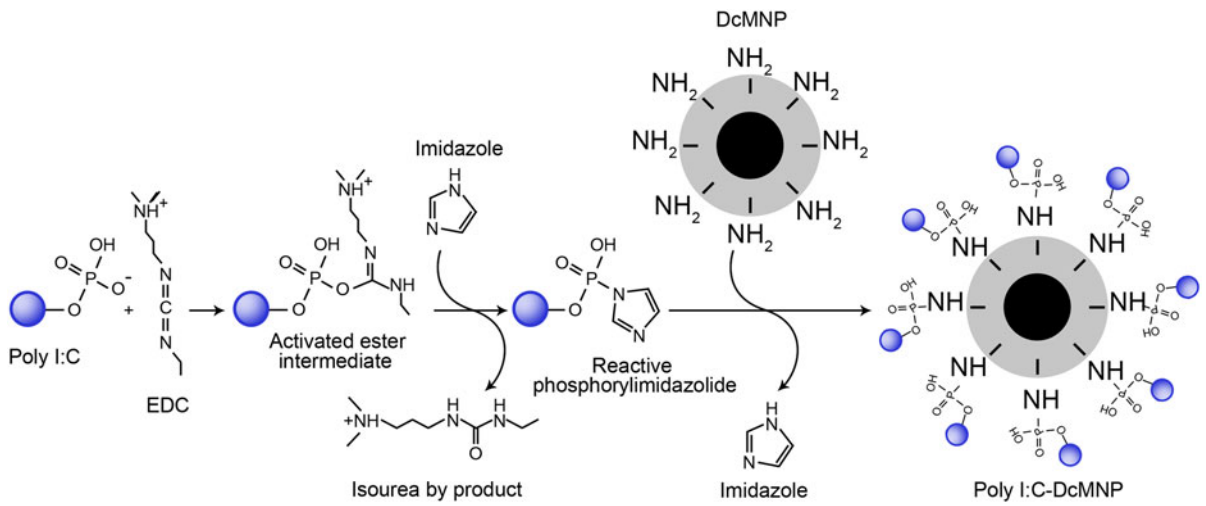

Fig. 3 Activation of Poly (I:C) by EDC and formation of phosphoramidate bond between phosphate group of Poly (I:C) and surface amine groups of DcMNPs

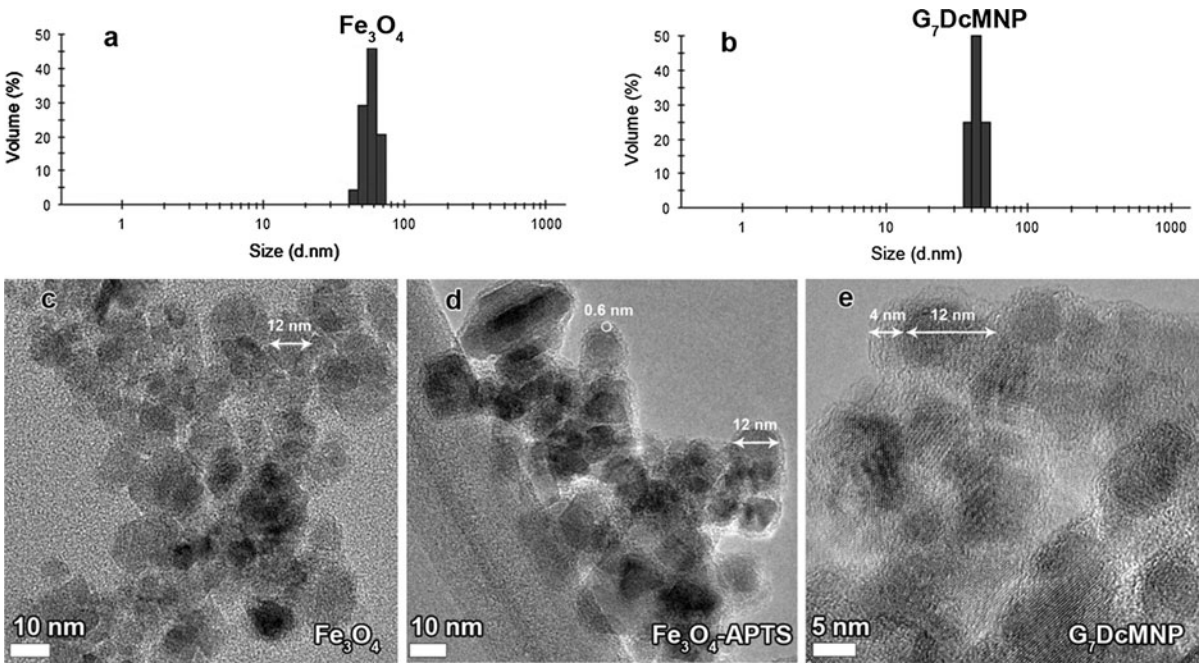

Fig. 4 Dynamic Light Scattering graphs of bare MNPs **a** and G_7DcMNPs **b**. TEM images of bare iron oxide **c**, APTS-modified iron oxide nanoparticles **d** and G7PAMAM dendron-coated magnetic nanoparticles **e**

(Fig. 4). The higher value of average size of DcMNP in DLS originates from the fact that DLS measures the hydrodynamic radii of the particles, which include the solvent layer at the interface (Tomalia et al. 1986). In Fig. 5, TEM results show that the sizes of Poly I:C—bound G_7DcMNP were in the range of 50 ± 20 nm. In addition, the nanoparticles were more dispersed after Poly (I:C) binding.

The loading efficiency was characterized by agarose gel electrophoresis. Figures 6 and 7 show the loading optimization on G_7DcMNP at pH 7.5 and pH 7. The results show that to achieve 100 % loading efficiency in 1-methylimidazole buffer at pH 7.5 and pH 7, the PIC:G_7DcMNP ratio needed to be as 1:35 and 1:30 in the reaction, respectively.

The loading efficiencies on G_2, G_3, and G_4DcMNPs were also studied at pH 7. When the same ratio of DcMNPs were used for other generations (G_2–G_4), it was observed that the loading efficiency of Poly (I:C) on G_2, G_3, and G_4DcMNPs was very low (Fig. 8).

When Poly (I:C) bounding was performed in 1-methylimidazole buffer at pH = 6, 100 % loading efficiency of Poly (I:C) was obtained when the PIC:DcMNP ratio was 1:11, and 1:15 for G_7DcMNP and G_6DcMNP, respectively (Fig. 9). However, for 100 % loading of Poly (I:C) on G_5DcMNP, it was needed to increase the PIC:DcMNP ratio to 1:18 (Fig. 10). When Poly(I:C) loading was performed in pH 6, the loading efficiency increased 3.5-fold compared to pH 7 and 8.

To obtain the loading efficiency of Poly (I:C) on other generations (G_2–G_6) of DcMNPs, the amount of DcMNP was tried to be kept proportional to the generation numbers. In order to achieve 100 % loading efficiency of Poly (I:C) for generation 7, 6, and 5, it was needed to keep the ratio of PIC:DcMNP as 1:11, 1:15, and 1:18 for G_7, G_6, and G_5DcMNPs, respectively. Loading efficiency of Poly (I:C) on G_4DcMNP was about 80 % when the PIC:DcMNP ratio was applied as 1:22 at pH 6; while even at 1:38 ratio for the same generation of DcMNP, the loading was almost zero when loading performed at pH 7 MeIm buffer. Due to the lower functional groups at the surface of G_3 and G_2DcMNPs, the loading efficiency were very low in these generations at pH 6 (Fig. 10).

The stability studies at different acidic pH (3, 4, 4.2, 4.4, 4.7, 6) conditions demonstrated that the bounding of Poly (I:C) to DcMNP surface functional groups were very stable at acidic pH. Poly (I:C)-DcMNPs complex were very stable at lyophilized or aqueous

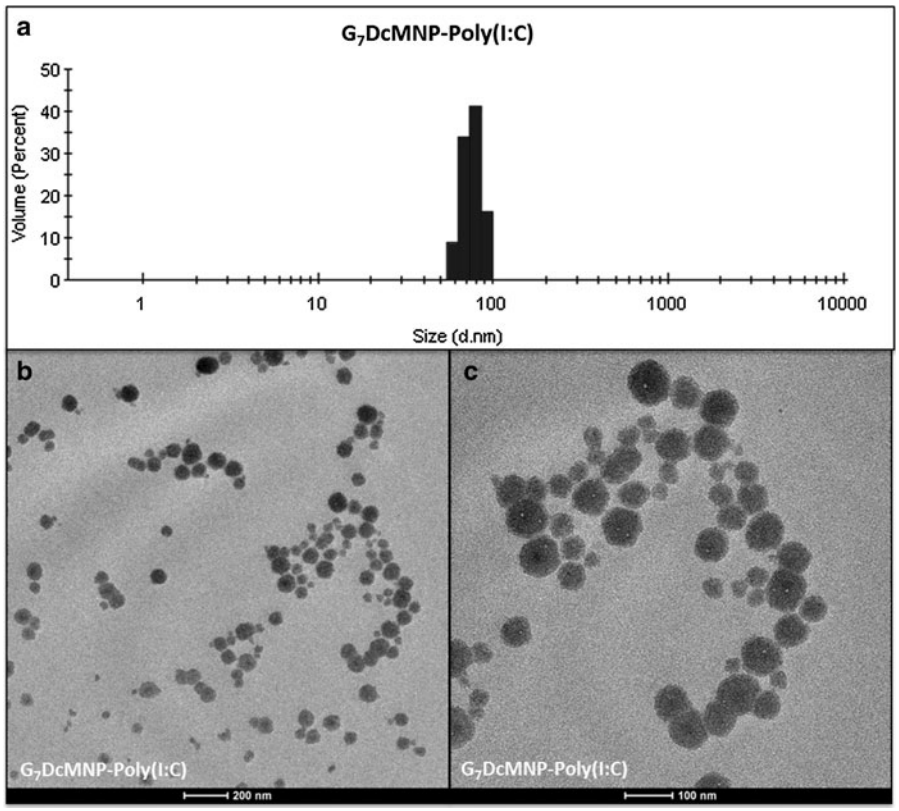

Fig. 5 Dynamic Light Scattering graphs of Poly (I:C) bounded G_7DcMNPs **a**. TEM images of Poly (I:C)-bounded G_7DcMNPs in 200 nm **b**, and 100 nm *scale bars* **c**

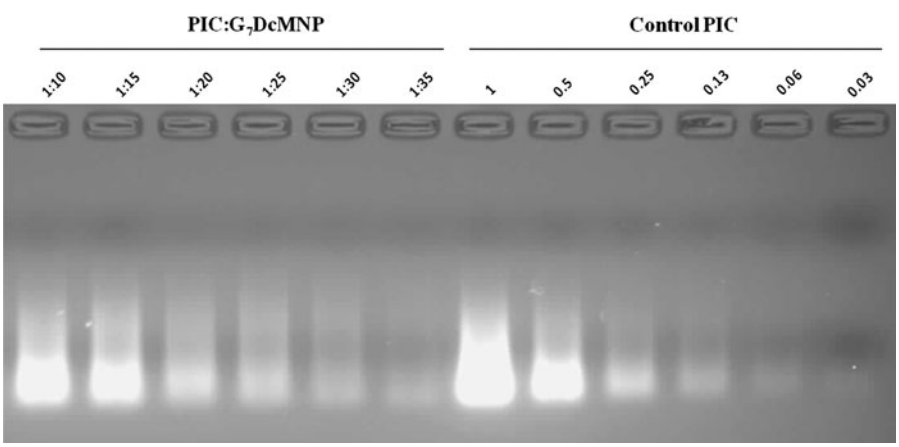

Fig. 6 Agarose gel electrophoresis of loading optimization 4 μg Poly (I:C) on G_7DcMNP at pH 7.5. Well 1, 2, 3, 4, 5, and 6 contain 1:10, 1:15, 1:20, 1:25, 1:30, and 1:35 ratio of Poly (I:C) :G_7DcMNP, respectively. Well 7 contains control Poly (I:C) and wells 8, 9, 10, 11, and 12 contain 1/2, 1/4, 1/8, 1/16, and 1/32 dilution of control Poly (I:C), respectively. 1 in the ratio represents 4 μg of Poly I:C or DcMNP

forms in both injection water and 1-methylimidazole buffer when stored at −20 °C up to 4 weeks. In addition, the complex was stable at high temperature (75 °C, 5 min) (data not shown).

The phosphoramide bound between Poly(I:C) and amine functional groups at the surface of DcMNPs were very sensitive to basic pH. The bond hydrolysis starts at pH 8.5 and the maximal hydrolysis was achieved at pH 9.4 for all generations. At pH 9.4, the half-life of the bound between Poly (I:C) and amine functional groups at the surface of DcMNPs was obtained as 15 min (data not shown). At pH 9 ± 0.2 after 1 h, the release amount was around 25 % and the half-life was 1 h. At generation 2 due to the low Poly (I:C) loading efficiency, the release amount was also low with respect to the other generations (Fig. 11).

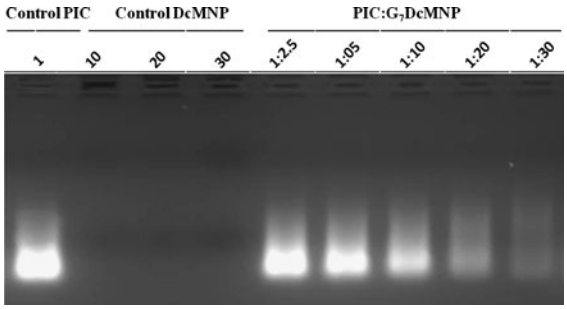

Fig. 7 Agarose gel electrophoresis of loading optimization of 4 μg Poly (I:C) on G_7DcMNP at pH 7. In first, well 4 μg Poly (I:C) was loaded as control. Wells 2, 3, and 4 contain 40 μg, 80 μg, and 120 μg G_7DcMNP, respectively. The wells 5–9 contain 1:2.5, 1:5, 1:10, 1:20, and 1:30 ratio of Poly (I:C) :G_7DcMNP, respectively. 1 in the ratio represents 4 μg of Poly I:C or DcMNP

Discussion

The immobilization of Poly (I:C) onto nanoparticles is an important tool for the fabrication of functional therapeutic materials (Shukoor et al. 2007; Khodadust et al. 2013; Pan et al. 2007). Due to their rapid clearance by nucleases, there is a need for carrier systems for Poly (I:C) treatment (Fischer et al. 2009). Untargeted Poly (I:C) has already been applied as adjuvants in cancer-directed human immunotherapy studies but by far not all applications (Okada 2009; Butowski et al. 2009; Jasani et al. 2009).

To have a successful therapeutic potential in cancer treatment, Poly (I:C) has to be delivered intracellularly into endosomes and also to the cytosol, in a tumor-targeted fashion. Up to now, both liposomal and polymer-based strategies have been developed which include antibody-targeted or pH-sensitive liposomes (Milhaud et al. 1989, 1992). In one of the studies, linear polyethylenimine-based polymeric carrier was found as most effective in Poly (I:C)-triggered killing of tumor cells which overexpress EGF-receptor (Schaffert et al. 2011). In addition, combination of mushroom derived polysaccharide and Poly (I:C)

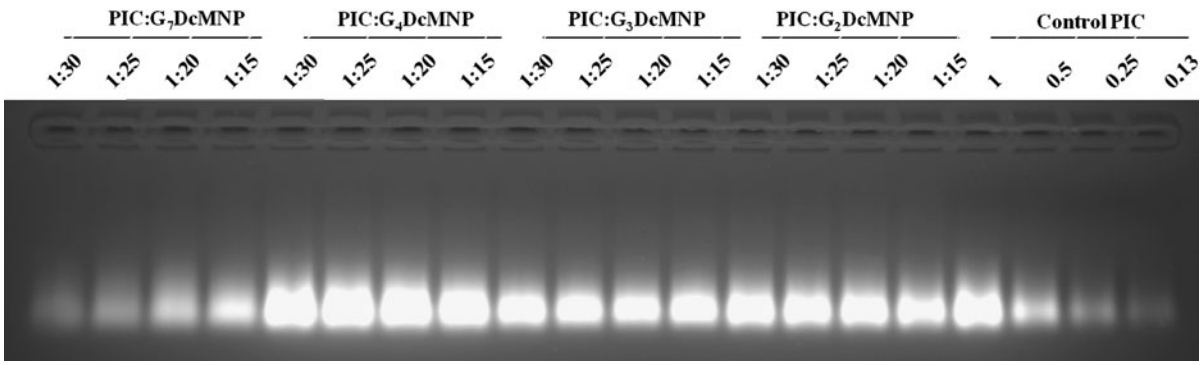

Fig. 8 Agarose gel electrophoresis of loading optimization Poly (I:C) on G_7, G_4, G_3, and G_2DcMNPs at pH 7. Wells 1–16 show the Poly (I:C) loading on G_7, G_4, G_3, and G_2DcMNPs at four different ratio. Wells 17–20 show the control Poly (I:C) and different dilutions. 1 in the ratio represents 4 μg of Poly I:C or DcMNP

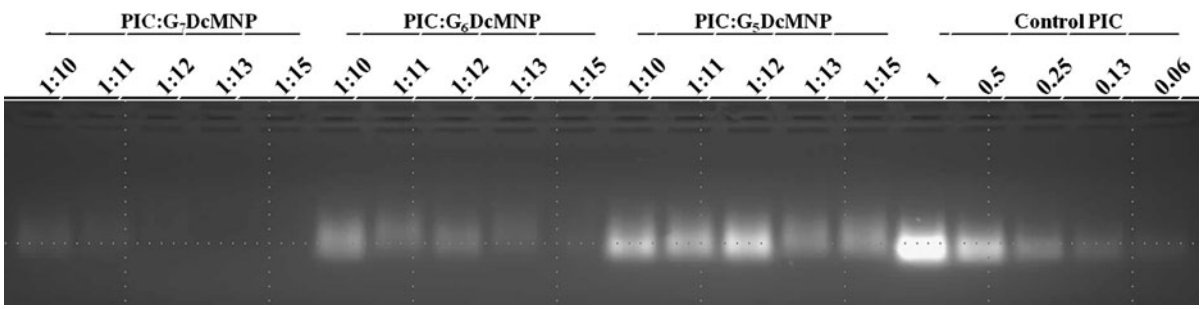

Fig. 9 Agarose gel electrophoresis of loading optimization Poly (I:C) on G_7, G_6, and G_5DcMNPs at pH 6. The ratio of Poly (I:C) to G_7, G_6, and G_5DcMNP was changed from 1:10 to 1:15. Wells 16–20 show the Poly (I:C) control and different dilutions. 1 in the ratio represents 4 μg of Poly I:C or DcMNP

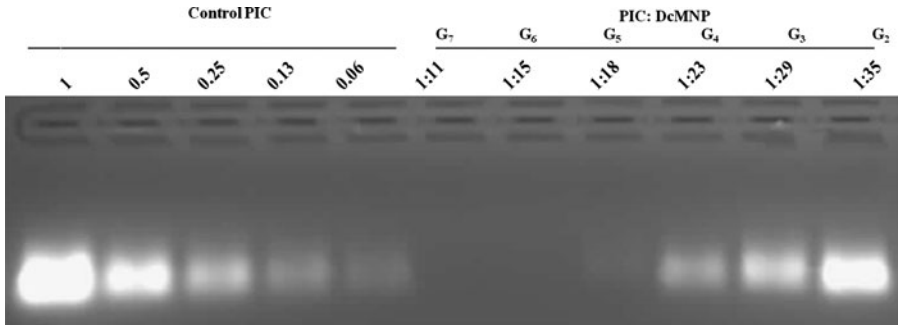

Fig. 10 Agarose gel electrophoresis of loading optimization Poly (I:C) on G_7, G_6, G_5, G_4, G_3, and G_2DcMNPs at pH 6. Wells 1–5 demonstrate the control Poly (I:C) and different dilutions. Wells 6–11 show the PIC:DcMNP ratio of G_7, G_6, G_5, G_4, G_3, and G_2DcMNPs. 1 in the ratio represents 4 μg of Poly I:C or DcMNP

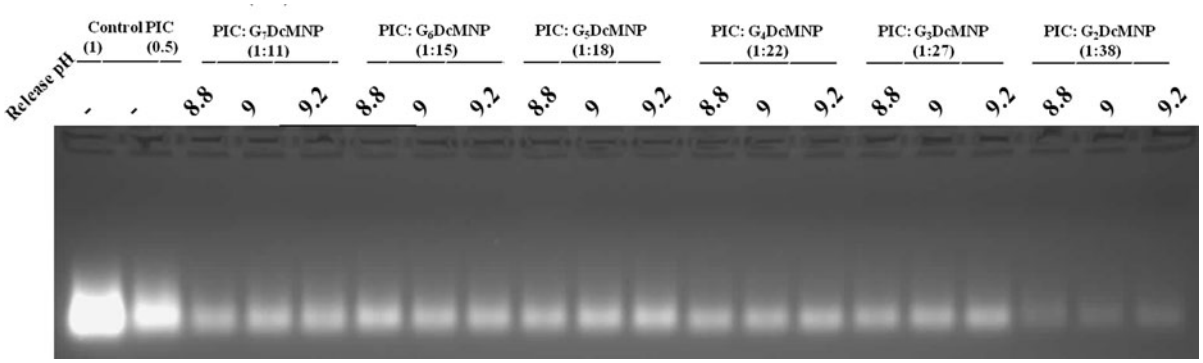

Fig. 11 Agarose gel electrophoresis of release study of Poly (I:C) on G_7, G_6, G_5, G_4, G_3, and G_2DcMNPs at pH 8.8, 9.0, and 9.2 for each generation, respectively. 1 in the ratio represents 4 μg of Poly I:C or DcMNP

forms stable nanocomplexes and triggers upregulation of inflammatory cytokines in another study (Tincer et al. 2011). Recently, cationic lipid-coated calcium phosphate nanoparticles constructed for co-delivery of zoledronic acid and Poly (I:C) was shown to have a better antitumor activity both in vitro and in vivo (Chen et al. 2013).

Magnetic nanoparticles are popular candidates for several biological applications including targeted cancer therapy studies since they can be targeted to the tumor site under magnetic field (Colombo et al. 2012; Widder et al. 1979). However, up to now, there are limited number of reports about the loading studies of the Poly (I:C) on magnetic nanoparticles. Initially, Shukoor et al. loaded Poly (I:C) onto γ-Fe_2O_3 nanoparticles through multifunctional polymeric ligand as a tool for targeting toll-like receptors (Shukoor et al. 2007, 2008). Recently, Poly (I:C) has been loaded on gold nanoparticles using PEG bio-functional spacers and TAT peptide (Sanz et al. 2012).

In this study, different generations of newly synthesized PAMAM-dendron-coated magnetic nanoparticles which can be targeted to the tumor site under magnetic field were efficiently loaded for the first time with Poly (I:C) in order to enhance Poly (I:C) action at the tumor site. The optimum loading efficiencies and stabilities at different pH conditions were discussed.

Previously, Shukoor et al. loaded Poly (I:C) on γ-Fe_2O_3 nanoparticles using multifunctional polymeric ligand at pH 7.5 (Shukoor et al. 2007). In this study, it was tried to optimize the maximum loading efficiency condition for Poly (I:C) on PAMAM DcMNPs using different pH conditions. By studying different pH (6, 7 and 7.5) values, it was obtained that the loading efficiency of Poly (I:C) on DcMNPs were almost similar at pH 7 and 7.5 for generation 7. However, at pH 6 the loading efficiency of Poly (I:C) on G_7DcMNPs were 3.5-fold higher than that of pH 7 and 7.5. At pH 7 MeIm buffer Poly (I:C) was not loaded on G_4DcMNPs even when the G_4DcMNP ratio increased up to 35-fold

with respect to Poly (I:C). However, at pH 6 MeIm buffer, the loading efficiency of Poly(I:C) was obtained as about 80 % when the PIC:G_4DcMNP ratio was 1:22. Although, unlike at pH 7 and pH 7.5, Poly (I:C) was also loaded on lower generations (G_3 and G_2DcMNPs) at pH 6, the loading efficiency was very low in these generations due to the small numbers of functional groups at the surface. These results contributed that loading of Poly (I:C) onto PAMAM DcMNPs at acidic pH was superior to neutral and basic pH. Yi Liu et al. demonstrated that pH-induces conformational change of PAMAM dendrimers from a "dense core" (high pH) to a "dense shell" (low pH) (Liu et al. 2009). Therefore at acidic pH, the surface amine functional groups of PAMAM dendrons would be more prone for Poly (I:C) binding than in basic and neutral pH. Results of this study confirm that efficient binding of Poly (I:C) on DcMNPs was performed when the activation and loading were performed at acidic pH. In addition, according to the literature nucleic acids should be activated in the presence of EDC at acidic pH for an efficient binding with amine and carboxyl groups (Sheehan et al. 1961). Thereby, higher loading efficiency may also be partly related to the activation condition by EDC.

The phosphoramide bound between Poly (I: C) and amine functional groups at the surface of DcMNPs were very sensitive to basic pH. In this study, it was demonstrated that the phosphoramide bound between the Poly I:C-DcMNPs complex is stable at acidic condition up to pH:3 values. On the other hand, at pH 8.5 the bound between Poly (I:C) and DcMNPs starts to be hydrolyzed, and the maximal hydrolysis was achieved at pH 9.4. The half-life of the bond between Poly (I:C) and surface amine groups of DcMNPs at pH 9.4 was obtained as 30 min. Poly(I:C)-DcMNPs bound was shown to be highly stable in powder form and aqueous form when stored at pH 6 (MeIm buffer), and pH 7 (PBS buffer and injection water) up to 4 weeks. These results demonstrate that the storage of the Poly I:C-DcMNPs complex is safe in powder form, or in aqueous form at acidic to neutral pH.

Recent findings demonstrated that dendrimers can cross cell membranes by endocytosis (Seib et al. 2007). The release of Poly (I:C) from DcMNPs was not related to pH when the nanoparticles are inside the cells. Poly (I:C) is on the surface of DcMNPs where it can bind to receptors efficiently without its release. In endosome, the Poly (I:C) at the surface of DcMNPs will bind to TLR3 receptors and induce apoptosis. In the case of their diffusion to the cytoplasm, eventually they will bind to the cytoplasmic receptors of Poly (I:C) which are MDA-5 and RIG-1 proteins. This binding will activate some apoptotic proteins like PUMA and NOXA (Xiangzhong et al. 2012; Kato et al. 2006).

In 1984, it was reported that the phophoamidase enzyme hydrolysis the bond between P and N in phosphoramide. Hystochemical study for the demonstration of sites of phosphamidase activity showed that small amounts of the enzyme are present in many normal tissues; however, large amounts are found in the gray matter of the central nervous system and in malignant epithelial tumors (Gomori 1948; Friedman et al. 1954; Meyer and Weinmann 1957; Ludeman 1999). Therefore, in case of application for siRNA delivery, the phosphoramide bindings between phosphates group of siRNA and amine groups of DcMNPs will be hydrolyzed by phosphoramidase enzymes which are especially active in malignant cancer cells.

In conclusion, this is a novel optimization study of Poly (I:C) loading onto different generations of PAMAM dendron-coated magnetic nanoparticles. Higher generations (G_7, G_6, G_5) due to more functional groups at their surface were more suitable to be used as a delivery system for Poly (I:C). In addition, acidic conditions of the reaction were superior to basic and neutral for the binding of Poly (I:C) on different generations of DcMNPs. Site-specific delivery of therapeutics can significantly reduce the potential toxicity and increase the therapeutic effects. Further in vitro and in vivo analysis of these Poly I:C/PAMAM DcMNP complexes will open up new opportunities for the selective marking of cells using magnetic properties of these nanoparticles.

Acknowledgments This study was supported by TÜBİTAK (TBAG-109T949 and TBAG-2215), and Middle East Technical University (BAP-07-02-2010-06).

Conflict of interest The authors declare that they have no conflict of interest.

References

Borges O, Silva M, de Sousa A, Borchard G, Junginger HE, Cordeiro-da-Silva A (2008) Alginate coated chitosan nanoparticles are an effective subcutaneous adjuvant for

hepatitis B surface antigen. Int Immunopharmacol 8:1773–1780

Bosman AW, Janssen HM, Meijer EW (1999) About dendrimers: structure, physical properties and applications. Chem Rev 99:1665–1688

Butowski N, Lamborn KR, Lee BL, Prados MD, Cloughesy T, DeAngelis LM, Abrey L, Fink K, Lieberman F, Mehta M, Ian Robins H, Junck L, Salazar AM, Chang SM (2009) A North American brain tumor consortium phase II study of poly-ICLC for adult patients with recurrent anaplastic gliomas. J Neurooncol 91:183–189

Chen L, Ding Y, Wang Y, Liu X, Babu R, Ravis W, Yan W (2013) Codelivery of zoledronic acid and doublestranded RNA from core–shell nanoparticles. Int J Nanomed 8:137–145

Colombo M, Carregal-Romero S, Casula MF, Gutiérrez L, Morales MP, Böhm IB, Heverhagen JT, Prosperi D, Parak WJ (2012) Biological applications of magnetic nanoparticles. Chem Soc Rev 41:4306–4334

Dobson J (2006) Magnetic nanoparticles for drug delivery. Drug Dev Res 67:55–60

Du X, Poltorak A, Wei Y, Beutler B (2000) Three novel mammalian toll-like receptors: gene structure, expression, and evolution. Eur Cytokine Netw 11:362–371

Esfand R, Tomalia DA (2001) Poly(amidoamine) (PAMAM) dendrimers: from biomimicry to drug delivery and biomedical applications. Drug Discov Today 6:427–436

Fischer S, Schlosser E, Mueller M, Csaba N, Merkle HP, Groettrup M, Gander B (2009) Concomitant delivery of a CTL-restricted peptide antigen and CpG ODN by PLGA microparticles induces cellular immune response. J Drug Target 17:652–661

Friedman OM, Klass DL, Seligman AM (1954) *N*-phosphorylated derivatives of diethanolamine1. J Am Chem Soc 76:916–917

Gao F, Pan BF, Zheng WM, Ao LM, Gu HC (2005) Study of streptavidin coated onto PAMAM dendrimer modified magnetite nanoparticles. J Magn Magn Mater 293:48–54

Gomori G (1948, December) Histochemical demonstration of sites of phosphamidase activity. In Proceedings of the society for experimental biology and medicine, Vol. 69, No. 3. Society for Experimental Biology and Medicine, Royal Society of Medicine, New York, p 407–409

Hansson GK, Edfeldt K (2005) Toll to be paid at the gateway to the vessel wall. Arterioscler Thromb Vasc Biol 25: 1085–1087

Hemmi H, Takeuchi O, Kawai T, Kaisho T, Sato S, Sanjo H, Matsumoto M, Hoshino K, Wagner H, Takeda K, Akira S (2000) A Toll-like receptor recognizes bacterial DNA. Nature 408:740–745

Ho KM, Li P (2008) Design and synthesis of novel magnetic core-shell polymeric particles. Langmuir 24:1801–1807

Jasani B, Navabi H, Adams M (2009) Ampligen: a potential toll-like 3 receptor adjuvant for immunotherapy of cancer. Vaccine 27:3401–3404

Kato H, Takeuchi O, Sato S, Yoneyama M, Yamamoto M, Matsui K, Uematsu S, Jung A, Kawai T, Ishii KJ, Yamaguchi O, Otsu K, Tsujimura T, Koh CS, Reis e Sousa C, Matsuura Y, Fujita T, Akira S (2006) Differential roles of MDA5 and RIG-I helicases in the recognition of RNA viruses. Nature 441:101–105

Kawai T, Akira S (2010) The role of pattern-recognition receptors in innate immunity: update on Toll-like receptors. Nat Immunol 11:373–384

Kawai T, Takahashi K, Sato S, Coban C, Kumar H, Kato H, Ishii KJ, Takeuchi O, Akira S (2005) IPS-1, an adaptor triggering RIG-I- and Mda5-mediated type I interferon induction. Nat Immunol 6:981–988

Khodadust R, Ünsoy G, Yalçın S, Gündüz G, Gündüz U (2013) PAMAM dendrimer-coated iron oxide nanoparticles:synthesis and characterization of different generations. J Nanopart Res 15:1488–1501

Khvalevsky E, Rivkin L, Rachmilewitz J, Galun E, Giladi H (2007) TLR3 signaling in a hepatoma cell line is skewed towards apoptosis. J Cell Biochem 100:1301–1312

Kohler N, Fryxell GE, Zhang M (2004) A bifunctional poly(ethylene glycol) silane immobilized on metallic oxide-based nanoparticles for conjugation with cell targeting agents. J Am Chem Soc 126:7206–7211

Kumar H, Kawai T, Kato H, Sato S, Takahashi K, Coban C, Yamamoto M, Uematsu S, Ishii KJ, Takeuchi O, Akira S (2006) Essential role of IPS-1 in innate immune responses against RNA viruses. J Exp Med 203:1795–1803

Liu Y, Bryantsev VS, Diallo MS, Goddard WA (2009) PAMAM dendrimers undergo pH responsive conformational changes without swelling. J Am Chem Soc 131:2798–2799

Ludeman SM (1999) The chemistry of the metabolites of cyclophosphamide. Curr Pharm Des 5:627–644

Maiti PK, Çağın T, Lin ST, Goddard WA (2005) Effect of solvent and pH on the structure of PAMAM dendrimers. Macromolecules 38:979–991

Matsumoto M, Funami K, Oshiumi H, Seya T (2004) Toll-like receptor 3: a link between toll-like receptor, interferon and viruses. Microbiol Immunol 48:147–154

McBain SC, Yiu HHP, Haj AE, Dobson J (2007) Polyethyleneimine functionalized iron oxide nanoparticles as agents for DNA delivery and transfection. J Mater Chem 17:2561–2565

Meyer J, Weinmann JP (1957) Occurrence of phosphamidase activity in keratinizing epithelia1. J Investig Dermatol 29:393–405

Milhaud PG, Machy P, Lebleu B, Leserman L (1989) Antibody targeted liposomes containing poly(rI).poly(rC) exert a specific antiviral and toxic effect on cells primed with interferons alpha/beta or gamma. Biochim Biophys Acta 987:15–20

Milhaud PG, Compagnon B, Bienvenue A, Philippot JR (1992) Interferon production of 1929 and hela cells, enhanced by polyriboinosinic acid-polyribocytidylic acid pH-sensitive liposomes. Bioconjug Chem 3:402–407

Mornet S, Vasseur S, Grasset F, Duguet E (2004) Magnetic nanoparticle design for medical diagnosis and therapy. J Mater Chem 14:2161–2175

Okada H (2009) Brain tumor immunotherapy with type-1 polarizing strategies. Ann NY Acad Sci 1174:18–23

Pan B, Cui D, Sheng Y, Ozkan C, Gao F, He R, Li Q, Xu P, Huang T (2007) Dendrimer-modified magnetic nanoparticles enhance efficiency of gene delivery system. Cancer Res 67:8156–8163

Patri AK, István JM, Baker JR (2002) Dendritic polymer macromolecular carriers for drug delivery. Curr Opin Chem Biol 6:466–471

Salaun B, Greutert M, Romero P (2009) Toll-like receptor 3 is necessary for dsRNA adjuvant effects. Vaccine 27: 1841–1847

Salem ML, El-Naggar SA, Kadima A, Gillanders WE, Cole DJ (2006) The adjuvant effects of the toll-like receptor 3 ligand polyinosinic-cytidylic acid poly (I:C) on antigen-specific CD8 + T cell responses are partially dependent on NK cells with the induction of a beneficial cytokine milieu. Vaccine 24:5119–5132

Salvador A, Igartua M, Hernandez RM, Pedraz JL (2012) Combination of immune stimulating adjuvants with poly(lactide-co-glycolide) microspheres enhances the immune response of vaccines. Vaccine 30:589–596

Sanz V, Conde J, Hernandez Y, Baptista PV, Ibarra MR, Fuente JM (2012) Effect of PEG biofunctional spacers and TAT peptide on dsRNA loading on gold nanoparticles. J Nanopart Res 14:917–925

Schaffert D, Kiss M, Rödl W, Shir A, Levitzki A, Ogris M, Wagner E (2011) Poly(I:C)-mediated tumor growth suppression in EGF-receptor overexpressing tumors using EGF-polyethylene glycol-linear polyethylenimine as carrier. Pharm Res 28:731–741

Schlosser E, Mueller M, Fischer S, Basta S, Busch DH, Gander B, Groettrup M (2008) TLR ligands and antigen need to be coencapsulated into the same biodegradable microsphere for the generation of potent cytotoxic T lymphocyte responses. Vaccine 26:1626–1637

Schulz O, Diebold SS, Chen M, Näslund TI, Nolte MA, Alexopoulou L, Azuma YT, Flavell RA, Liljeström P, Reis e Sousa C (2005) Toll-like receptor 3 promotes cross-priming to virus-infected cells. Nature 433:887–892

Seib FP, Jones AT, Duncan R (2007) Comparison of the endocytic properties of linear and branched PEIs, and cationic PAMAM dendrimers in B16f10 melanoma cells. J Control Release 117:291–300

Sheehan J, Cruickshank P, Boshart G (1961) A convenient synthesis of water-soluble carbodiimides. J Org Chem 26:2525

Shen T, Weissleder R, Papisov M, Bogdanov A, Brady TJ (1993) Monocrystalline iron oxide nanocompounds (MION): physicochemical properties. Magn Reson Med 29:599–604

Shir A, Ogris M, Wagner E, Levitzki A (2006) EGF receptor-targeted synthetic double-stranded RNA eliminates glioblastoma, breast cancer, and adenocarcinoma tumors in mice. PLoS Med 3(1):e6

Shukoor MI, Natalio F, Ksenofontov V, Tahir MN, Eberhardt M, Theato P, Schröder HC, Müller WE, Tremel W (2007) Double-stranded RNA polyinosinic-polycytidylic acid immobilized onto gamma-Fe2O3 nanoparticles by using a multifunctional polymeric linker. Small 3:1374–1378

Shukoor MI, Natalio F, Metz N, Glube N, Tahir MN, Therese HA, Ksenofontov V, Theato P, Langguth P, Boissel JP, Schröder HC, Müller WE, Tremel W (2008) dsRNA-functionalized multifunctional gamma-Fe2O3 nanocrystals: a tool for targeting cell surface receptors. Angew Chem Int Ed Engl 47:4748–4752

Sun C, Lee JS, Zhang M (2008) Magnetic nanoparticles in MR imaging and drug delivery. Adv Drug Deliv Rev 60:1252–1265

Svenson S, Tomalia DA (2005) Dendrimers in biomedical applications-reflections on the field. Adv Drug Deliv Rev 57:2106–2129

Tabeta K, Georgel P, Janssen E, Du X, Hoebe K, Crozat K, Mudd S, Shamel L, Sovath S, Goode J, Alexopoulou L, Flavell RA, Beutler B (2004) Toll-like receptors 9 and 3 as essential components of innate immune defense against mouse cytomegalovirus infection. Proc Natl Acad Sci USA 101:3516–3521

Takeda K, Kaisho T, Akira S (2003) Toll-like receptors. Annu Rev Immunol 21:335–376

Tincer G, Yerlikaya S, Yagci FC, Kahraman T, Atanur OM, Erbatur O, Gursel I (2011) Immunostimulatory activity of polysaccharide-poly(I:C) nanoparticles. Biomaterials 32:4275–4282

Tomalia DA, Baker H, Dewald J, Hall M, Kallos G, Martin S, Roeck J, Ryder J, Smith P (1986) Dendritic macromolecules: synthesis of starburst dendrimers. Macromolecules 19:2466–2468

Unsoy G, Yalcin S, Khodadust R, Gunduz G, Gunduz U (2012) Synthesis optimization and characterization of chitosan-coated iron oxide nanoparticles produced for biomedical applications. J Nanopart Res 14:964–977

Veiseh O, Gunn JW, Zhang M (2010) Design and fabrication of magnetic nanoparticles for targeted drug delivery and imaging. Adv Drug Deliv Rev 62:284–304

Weber A, Kirejczyk Z, Besch R, Potthoff S, Leverkus M, Häcker G (2010) Proapoptotic signalling through Toll-like receptor-3 involves TRIF-dependent activation of caspase-8 and is under the control of inhibitor of apoptosis proteins in melanoma cells. Cell Death Differ 17:942–951

Whitesides GM (2003) The 'right' size in nanobiotechnology. Nat Biotechnol 21:1161–1165

Widder KJ, Senyei AE, Ranney DF (1979) Magnetically responsive microspheres and other carriers for the biophysical targeting of antitumor agents. Adv Pharmacol Chemother 16:213–271

Xiangzhong Z, Miao A, Yuqi G, Xianbin Z, Li W, Xia L, Chengfang Y (2012) Poly I:C-ınduced tumor cell apoptosis mediated by pattern-recognition receptors. Cancer Biother Radiopharm 27:530–534